Microbial Cell Factories

RESEARCH

Open Access

Development and construction of a novel *Bacillus subtilis* autoinducible extracellular expression system based on a LuxI/R device

Bin Wang[1,2,3†], Keyi Wang[1,2,3†], Xiuyue Zhao[1,2,3], Zemin Fang[1,2,3], Yanyan Zhao[1,2,3], Yulu Fang[1,2,3], Yazhong Xiao[1,2,3*] and Dongbang Yao[1,2,3*]

Abstract

Background Microbial chassis expression systems are valuable tools in biotechnology and synthetic biology, and *Bacillus subtilis* is an important industrial microbial chassis. Quorum sensing (QS)-based dynamic regulation is widely used to automatically activate gene expression in response to changes in cell density. The main bottleneck currently limiting the use of exogenous QS systems in *B. subtilis* for efficient autoinducible extracellular expression of recombinant proteins is their low level of autoinducible expression.

Results A novel *B. subtilis* autoinducible extracellular expression system based on the LuxI/R-type QS system (*lux* system) of *Vibrio fischeri* was developed in which the autoinducible expression of the *lux* system was enhanced by engineering the sensing module and response module promoters. By engineering the sensing module promoter SP_{luxI} core region (−10 and −35 elements) and critical region (UP and spacer elements), and the response module promoter RP_{luxIR6} core region and *lux* box copy number in the original LuxI/R device (S0-R0), the high-expression Sc-R2 construct was obtained. After shake flask and 3-L fermenter fermentation, the extracellular amylase activity obtained with Sc-R2 was 2.7- and 3.1-fold greater, respectively, than that obtained with the well-characterized promoter P_{veg}. Sc-R2 achieved 2.6-fold greater extracellular activity than S0-R0 when either levansucrase or invertase was used as a reporter protein. Overall, the *B. subtilis* autoinducible extracellular expression system developed in this study showed good generalizability and application potential for industrial-scale fermentation.

Conclusions To our knowledge, this is the first study to report enhanced autoinducible expression of the *lux* system in *B. subtilis* by engineering the sensing module promoter SP_{luxI} sequence and the *lux* box copy number of the response module promoter RP_{luxIR6}. This study further expands the application potential of the *B. subtilis* expression system in synthetic biology.

Keywords *Bacillus subtilis*, Quorum sensing, *Lux* system, Autoinducible extracellular expression, Promoter

†Bin Wang and Keyi Wang contributed equally to this work.

*Correspondence:
Yazhong Xiao
yzxiao@ahu.edu.cn
Dongbang Yao
dbyaoanhui@ahu.edu.cn

[1]School of Life Sciences, Anhui University, Hefei 230601, China
[2]Anhui Key Laboratory of Biocatalysis and Modern Biomanufacturing, Hefei 230601, China
[3]Anhui Provincial Engineering Technology Research Center of Microorganisms and Biocatalysis, Hefei 230601, China

Background

Microbial chassis expression systems are valuable tools for biotechnology and synthetic biology. The efficient and precise expression of genes of interest (GOIs) is essential for the successful construction of microbial chassis expression systems that efficiently produce enzymes and other natural products [1]. GOIs can be expressed in either constitutive or inducible systems [2]. Compared with a constitutive system, an inducible system has significant application potential because of the ability to regulate the level and timing of GOI expression in such systems. In addition, inducible systems can decouple cell growth and GOI expression processes and thus overcome challenges related to limited resource allocation between these two processes [3]. Inducible microbial chassis expression systems include inducer-based and bacterial quorum sensing (QS)-based systems [4]. When using inducer-based expression systems, cell growth is monitored, and an inducer is added at the appropriate time [5]. This leads to increased labour and production costs, which limits the industrial application value of this type of system. Therefore, QS-based autoinducible expression systems have become a prominent research focus because of their ability to autonomously activate gene expression at specific cell densities without the need to add external inducers or monitor cell growth [6].

Bacillus subtilis has been developed into an important industrial microbial cell factory because of its robust protein synthesis and secretion capabilities, ease of cultivation, and generally regarded as safe (GRAS) designation [7]. It has been widely used to produce a variety of industrial enzymes, such as amylases and pullulanases [8, 9]. QS is a population density-dependent cell signalling mechanism [10]. The QS systems currently used in *B. subtilis* include the endogenous ComQXPA and Phr-Rap systems and the exogenous LuxI/R-type system (*lux* system) derived from *Vibrio fischeri* [11–13]. The autoinducer in the ComQXPA and Phr-Rap systems is an oligopeptide, also known as an autoinducible peptide [14], whereas the autoinducer in the *lux* system is acylhomoserine lactone (AHL) [15]. Currently, the autoinducible extracellular expression of recombinant proteins in *B. subtilis* relies on its endogenous ComQXPA-type QS system [6, 13, 16]. However, cell growth and the expression of recombinant proteins via endogenous systems may be hindered by interference from other cellular physiological processes [17]. In contrast, the exogenous *lux* system can overcome these issues because it is bioorthogonal to the natural QS system of *B. subtilis*.

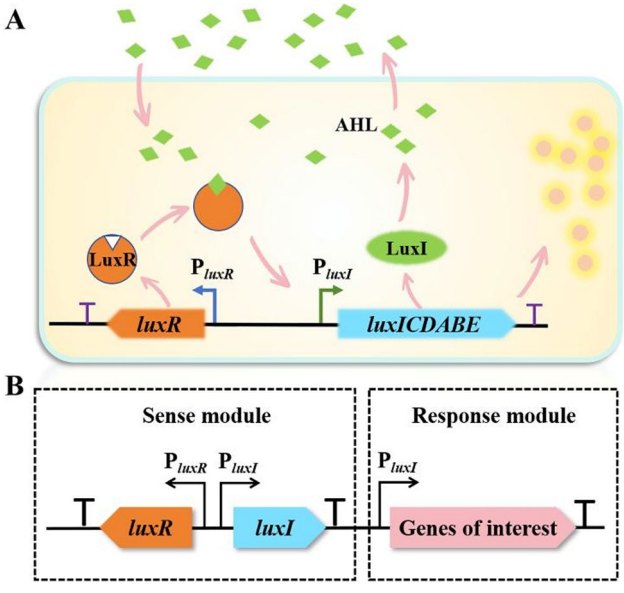

Fig. 1 Mechanism (**A**) and application (**B**) of the *lux*-type QS system

The *lux* system of *V. fischeri* consists of the *luxR* and *luxICDABE* operons, known as the LuxI/R device [18]. *luxR* encodes the AHL receptor protein LuxR, *luxI* encodes the AHL synthase LuxI, and *luxCDABE* encodes a bioluminescence-related protein (Fig. 1A). The N- and C-terminal domains of LuxR bind to AHL and the *lux* box region of the promoter P_{luxI}, respectively. All cells in the population produce AHL at a low basal level, and the AHL produced freely diffuses out of the cell. When the concentration of AHL reaches a specific threshold, AHL binds to the N-terminal domain of intracellular LuxR. This binding alleviates C-terminal domain inhibition by the N-terminal domain. The resulting LuxR – AHL complex subsequently binds to the *lux* box region of P_{luxI}. Then, RNA polymerase (RNAP) is recruited to increase the transcriptional activity of P_{luxI}, increasing the expression of the luminescence gene operon *luxICDABE*. This leads to an exponential rise in AHL production and cellular luminescence as the cells continue to grow.

It is widely recognized that decomposing complex systems into multiple simple modules can decrease their complexity and facilitate their reconstruction and characterization [19]. In recent years, researchers have decomposed the *lux* system into a sensing module containing *luxI* and *luxR* and a response module in which P_{luxI} mediates the expression of a GOI (Fig. 1B), and the *B. subtilis* autoinducible expression system was constructed on the basis of these modules [11, 17]. Corrêa et al. demonstrated that the *lux* system functioned efficiently during the exponential growth phase of cells, with only minimal leakage of expression observed in the lag phase [17]. This closely matches the ideal pattern of protein expression [20]. These results suggest that the *lux* system has significant potential for autoinducible extracellular expression of recombinant proteins in *B. subtilis*. However, to our knowledge, there are no reports of autoinducible extracellular expression of recombinant proteins in *B. subtilis* via the *lux* system. The main reason for this is

that recombinant protein expression using the QS system requires high autoinducible expression [13], whereas the *lux* system exhibits low expression in *B. subtilis* [17]. Consequently, increasing the autoinducible expression of the *lux* system in *B. subtilis* is highly important.

As reported in previous studies, the autoinducible expression of the *lux* system in *B. subtilis* was enhanced only by increasing P_{luxI} transcriptional activity or by stabilizing the mRNAs of target genes in the response module. For example, Corrêa et al. increased the autoinducible expression of a *lux* system 154-fold by optimizing the sequence located between the − 35 region and the transcription start site of P_{luxI} in the response module [17]. In addition, Zhou et al. introduced random mutations in a sequence located within 4 bp upstream of the − 10 region of P_{luxI} in the response module [21]. The resulting mutant P58 exhibited a 1.39-fold increase in the expression of sfGFP in *B. subtilis* [21]. However, to our knowledge, there are no reports of the autoinducible expression of the *lux* system in *B. subtilis* being increased by engineering the sensing module.

The primary objective of this study was to enhance the autoinducible expression of the *V. fischeri lux* system in *B. subtilis* by engineering the sensing module and response module promoters and then further developing a novel and efficient *B. subtilis* autoinducible extracellular expression system regulated by the optimized LuxI/R device. In the initial experiments, an autoinducible extracellular expression system regulated by the LuxI/R device was constructed [22]. The autoinducible expression of the *lux* system in *B. subtilis* was then enhanced by engineering the core and critical regions in the sensing module promoter, and the core region and *lux* box copy number in the response module promoter. Finally, the generalizability and industrial-scale fermentation potential of the constructed *B. subtilis* autoinducible expression system were evaluated on the basis of the performance for three reporter proteins and in a 3-L fermenter, respectively.

Materials and methods

Strains, plasmids, and media

All strains and plasmids used in this study are listed in Additional file 1: Table S1. *B. subtilis* WB600 [23] was used as the host strain for plasmid construction and expression. LB medium and 2×YT medium containing 10 mM Ca^{2+} were used for seed culture and shake flask fermentation, respectively [8]. For fermentation in a 3-L fermenter, the basic medium contained 5 g/L molasses, 8.5 g/L soybean peptone, 5 g/L NaCl, 25.5 g/L yeast extract, 3 mL/L trace element solution [22], and 3 mM Ca^{2+}. The feed medium contained 360 g/L molasses, 30 g/L soybean peptone, 5 g/L NaCl, 90 g/L yeast extract, and 30 mL/L trace element solution.

Fermentation of *B. subtilis* in shake flasks and fermenters in this study was performed according to our previously reported methodology [8]. Briefly, for shake flask fermentation, a single colony selected from a Petri dish was first inoculated into a test tube containing 5 mL of LB medium. After overnight growth at 37 °C with shaking at 200 rpm, the culture was inoculated into a 250-mL shake flask containing 100 mL of 2×YT medium (2%, v/v) and incubated for 48 h at 30 °C with shaking at 200 rpm. For fermentation in 3-L fermenters, seed cultures were first obtained by growing a single colony in 60 mL of 2×YT medium at 37 °C with shaking at 200 rpm for 12 h. The culture was then inoculated into a 3-L fermenter (Eppendorf BioFlo 115, New Brunswick Scientific, USA) containing 1.2 L of the basic medium (5%, v/v). The dissolved oxygen content was maintained at approximately 30% by automated adjustment of the stirrer speed and air flow. The fermentation temperature was maintained at 30 °C, and the pH was maintained at 6.5–7.5 by adding NH_4OH and HCl as needed.

Plasmid construction and transformation

The primers used in this study are shown in Additional file 1: Table S2. The pBA-*luxI/R* fragment (the backbone of pBLA) was obtained from the plasmid pBHYCO6 [22] using the primers F1/R1. The T_{luxR}-*luxR*-SP_{luxR}-SP_{luxI}-*luxI*-T_{ter}-RP_{luxIR6} fragment was obtained from the plasmid pUC57-*luxI/R* using the primers F2 and R2. The plasmid pBLA was created by linking the T_{luxR}-*luxR*-SP_{luxR}-SP_{luxI}-*luxI*-T_{ter}-RP_{luxIR6} fragment with the pBA-*luxI/R* fragment using prolonged overlap extension polymerase chain reaction (POE-PCR) [24]. The pBA-*veg* fragment (the backbone of pBVA) was obtained from the plasmid pBHYCO6 [22] using the primers F3/R3. The promoter P_{veg} was obtained from the plasmid pBHZ-V [8] using the primers F4 and R4. The plasmid pBVA was created by linking P_{veg} with the pBA-*veg* fragment using POE-PCR. Sequence information for the T_{luxR}-*luxR*-SP_{luxR}-SP_{luxI}-*luxI*-T_{ter}-RP_{luxIR6} fragment and the promoter P_{veg} is provided in Additional file 1: Sequence information. The other plasmids used in this study were constructed in a similar manner, and the detailed procedures are described in Additional file 1: Plasmid construction. The methods used in this study for *B. subtilis* receptor cell preparation and plasmid transformation were described in our previously reported study [8].

Directed evolution of the response module promoter RP_{luxIR6} core region

B. subtilis WB600 transformants containing pBLA-RP_{luxIR6}′, in which RP_{luxIR6}′ represents a RP_{luxIR6} mutant library, were inoculated into 96-well plates (purchased from Shanghai Ganwei Biotechnology Co., Ltd., China) containing 600 μL of 2×YT medium supplemented with

10 mM Ca^{2+} and 30 μg/mL kanamycin and incubated at 30 °C with shaking at 700 rpm for 48 h. The fermentation supernatant was obtained by centrifugation of the fermentation cultures at 300 rpm for 10 min at 4 °C. Our previous OD_{600} measurement results for the 96-well plate fermentation system revealed that there was no significant difference in the OD_{600} values of the strains in the different wells, which were all in the range 5.9–7.1. For the sake of efficiency and simplicity, we did not adjust the OD_{600} values of the strains before centrifugation. The fermentation supernatant was inoculated onto plates containing 2% soluble starch and 1% agar and incubated at 30 °C for 2 h. The extracellular AmyZ1 activity of the transformants was assessed by measuring the diameter of the transparent circle after iodine staining.

Transformants with a transparent circle diameter significantly larger than that of the control WBLA were subjected to shake flask fermentation and then rechecked for AmyZ1 activity using the fermentation supernatant. Shake flask fermentation was performed by transferring the seed cultures into 250-mL shake flasks at 2% (v/v) in 100 mL of 2×YT medium. Cell lysis may have affected the results of the enzyme activity assay; however, the directed evolution of RP_{luxIR6} was performed using AmyZ1, which has high specific activity, as a reporter protein [25]. Therefore, the amounts of extracellular protein generated by the mutant and wild-type RP_{luxIR6}-regulated recombinant AmyZ1 showed little difference via sodium dodecyl sulfate–polyacrylamide gel electrophoresis (SDS–PAGE). Therefore, AmyZ1 protein expression levels were not further validated by SDS–PAGE. Finally, the sequence information of the promoter RP_{luxIR6}' corresponding to the transformants showing high extracellular AmyZ1 activity was obtained through sequencing.

Cell concentration and enzyme activity determination

The methods used in this study to determine the cell concentration and AmyZ1 activity were described in our previously reported study [8]. The method for determining invertase activity was modified from Liu et al. [26]. Briefly, 50 μL of a crude enzyme solution was added to a system containing 430 μL of citrate-disodium phosphate buffer (50 mmol/L, pH 6.5) and 120 μL of sucrose (final concentration of 2%). The mixture was then mixed well and incubated at 35 °C for 10 min. Then, 300 μL of 3,5-dinitrosalicylic acid (DNS) was added to stop the reaction. The mixture was boiled at 100 °C for 10 min, and the absorbance of the mixture was measured at 540 nm. One unit of enzyme activity (U) was defined as the amount of enzyme required to produce 1 μmol of glucose per minute under the above conditions. The levansucrase activity was determined via the method used to determine invertase activity.

Quantitative real-time PCR (qRT–PCR)

The method used to determine the *amyZ1* transcript levels in this study was described in our previous report [8]. The 16 S rRNA gene was used as the reference gene. The primers F5 and R5 and the primers F6 and R6 were used for qRT−PCR amplification of the *amyZ1* and 16 S rRNA genes, respectively (Additional file 1: Table S2). The transcript level of *luxI* was determined using a method similar to that used for *amyZ1*, wherein the qRT−PCR amplification primers for *luxI* were F7 and R7 (Additional file 1: Table S2). The data were analysed using the $2^{-\Delta\Delta CT}$ method [27].

Statistical analysis

All data in this study represent the mean (± standard deviation) of three independent experiments. The data were statistically analysed using Student's *t* test. Only differences with *p* values less than 0.05 were considered statistically significant.

Results and discussion

Development of a LuxI/R device-based autoinducible extracellular expression system for *B. subtilis*

The recombinant vector pBLA (Fig. 2A), comprising a sensing module with *luxI-luxR* and a response module with P_{luxIR6}-regulated *amyZ1* (encoding the raw starch-degrading α-amylase AmyZ1), was constructed [8]. In the LuxI/R device, the promoter for *luxI* in the sensing module is P_{luxI} (abbreviated as SP_{luxI}), and the promoter of *amyZ1* in the response module is R6 (abbreviated as RP_{luxIR6}) [17]. Then, pBLA was transformed into *B. subtilis* WB600 to obtain the recombinant strain WBLA. Compared with the autoinducible expression mediated by endogenous QS systems (e.g., the ComQXPA system), the current industrial use of *B. subtilis* as a chassis for efficient expression of recombinant proteins is based mainly on constitutive promoters. P_{veg} is a strong constitutive promoter commonly used in the *B. subtilis* expression system [28]. To increase the efficacy of industrial application of the *B. subtilis* autoinducible extracellular expression system based on the LuxI/R device, P_{veg} was chosen as the control in this study, and the control strain WBVA was constructed on the basis of the recombinant vector pBVA containing P_{veg} (Fig. 2A). To evaluate the production performance of the autoinducible extracellular expression system regulated by the LuxI/R device, shake flask fermentation was conducted with WBLA and WBVA, and the results were analysed.

As depicted in Fig. 2B and C, the WBLA and WBVA strains presented distinct correlations between extracellular amylase activity and the OD_{600}. The trend for the extracellular amylase activity of WBLA was similar to that for its OD_{600}, which was consistent with the design concept for QS system-mediated autoinducible

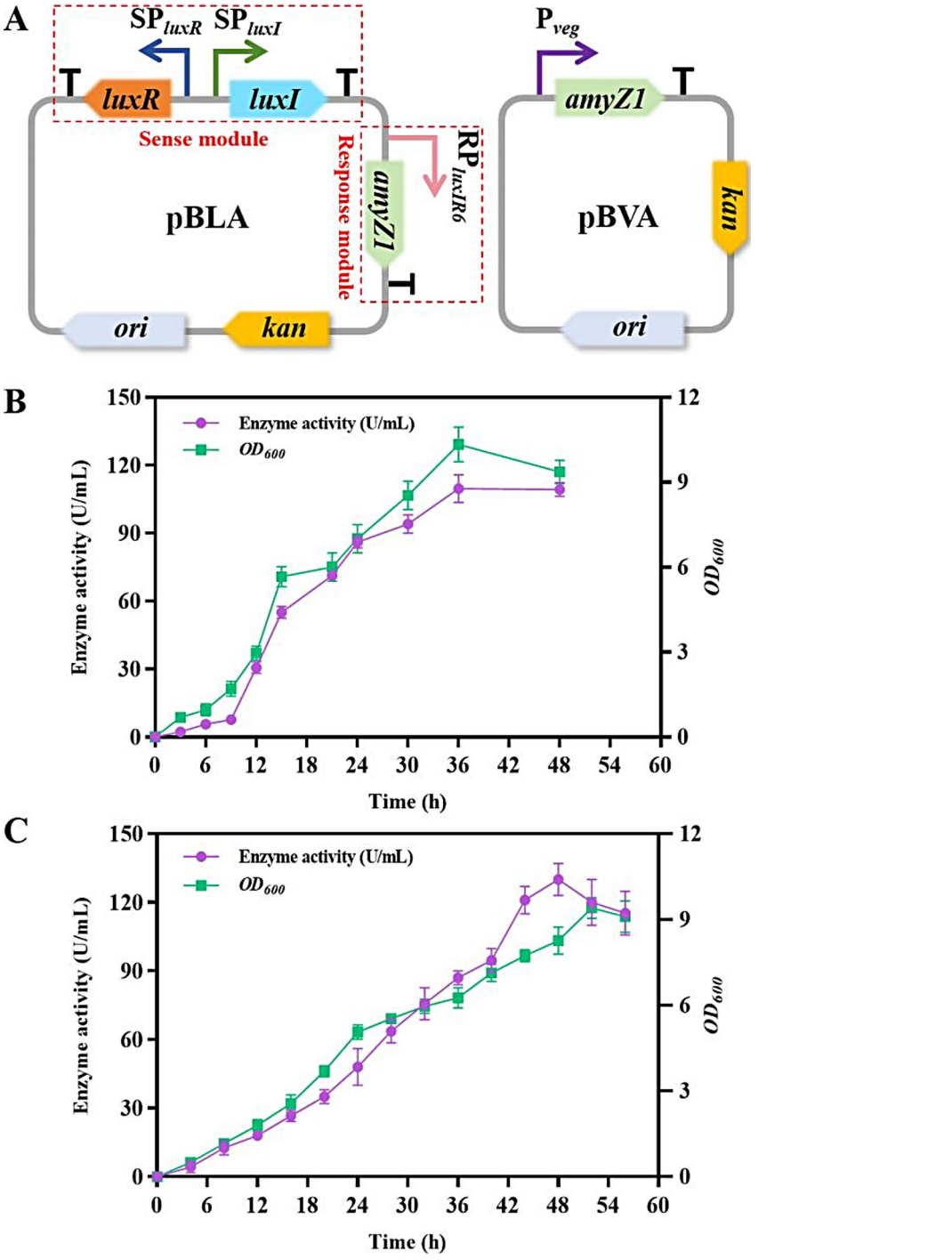

Fig. 2 The LuxI/R device and P_{veg} mediate extracellular expression of recombinant *amyZ1* in *B. subtilis*. (**A**) Plasmid profiles of pBLA and pBVA. Shake flask fermentation profiles of WBLA (**B**) and WBVA (**C**). The error bars represent the standard deviation

expression. After 36 h of culture, the OD_{600} and extracellular amylase activity of WBLA peaked at 10.2 and 115 U/mL, respectively, with a production efficiency of 3.2 U/mL·h. The OD_{600} and extracellular amylase activity of WBVA peaked at 51 and 48 h, with values of 9.4 and 130 U/mL, respectively, with a corresponding production efficiency of 2.7 U/mL·h. The OD_{600} and extracellular amylase activity of WBVA at 36 h were 6.2 and 87 U/mL, respectively, which were 39% and 24% lower than those of WBLA. This may be attributed to the fact that the autoinducible expression mediated by the LuxI/R device effectively alleviated the inverse relationship between cell growth and product synthesis.

In addition, the maximum extracellular amylase activity of WBVA was 1.13 times ($p < 0.05$) greater than that of WBLA, indicating a lower level of autoinducible expression mediated by the *lux* system in *B. subtilis* than in P_{veg}. Subsequent experiments focused on enhancing the autoinducible expression of the *lux* system by engineering the sensing module promoter SP_{luxI} and the response module promoter RP_{luxIR6}.

Engineering the −10 and −35 regions of SP_{luxI}

The −10 and −35 regions of the promoter function as recognition and binding sites for the σ factor of RNAP, which is the core region influencing its level of transcriptional activity [29]. Previous studies have demonstrated that engineering the −10 and −35 regions of a promoter effectively enhances transcriptional activity [17, 30, 31]. For example, by replacing the −35 region of P_{srfA} with the consensus sequence of the *B. subtilis* σ^A factor, the resulting mutant P1 exhibited an 85% increase in transcriptional activity [13]. In a previous study by Hu et al., the fluorescence intensities obtained with the mutants P_{D4} and P_{D7}, which were obtained by replacing the core region of the promoter P_{degQ} with the conserved recognition sequences σ^A, σ^B, and σ^H, were 3.6- and 2.8-fold greater, respectively, than those obtained with P_{degQ} [12]. Guan et al. used a similar method to modify the −10 region of P_{srfA}, producing the mutant P12, which presented a GFP fluorescence intensity that was 1.83-fold greater than that of the control P_{srfA} (P03) [31]. Here, we generated a series of promoter mutants (Fig. 3A) by replacing the −10 and −35 regions of SP_{luxI} with those from strong promoters commonly utilized in the *B. subtilis* expression system (P_{ylB} [3], P_{HpaII} [32], P_{43} [33], P_{spoVG} [34], P_{veg} [35], and P_{srfA} [36]). In theory, the core region of SP_{luxI} can be optimized by selecting these promoters as reference objects to generate mutants with increased expression of the GOI.

Figure 3A illustrates the significant differences in the extracellular amylase activity of the promoter mutants. The mutants $SP_{luxI-spoVG10}$, $SP_{luxI-4310}$, and $SP_{luxI-veg10}$ were obtained by replacing the −10 region of P_{spoVG}, P_{43}, and P_{veg}, respectively. These mutants exhibited extracellular amylase activities of 141, 143, and 134 U/mL (Fig. 3A), which were 1.23-, 1.24-, and 1.17-fold ($p < 0.05$)

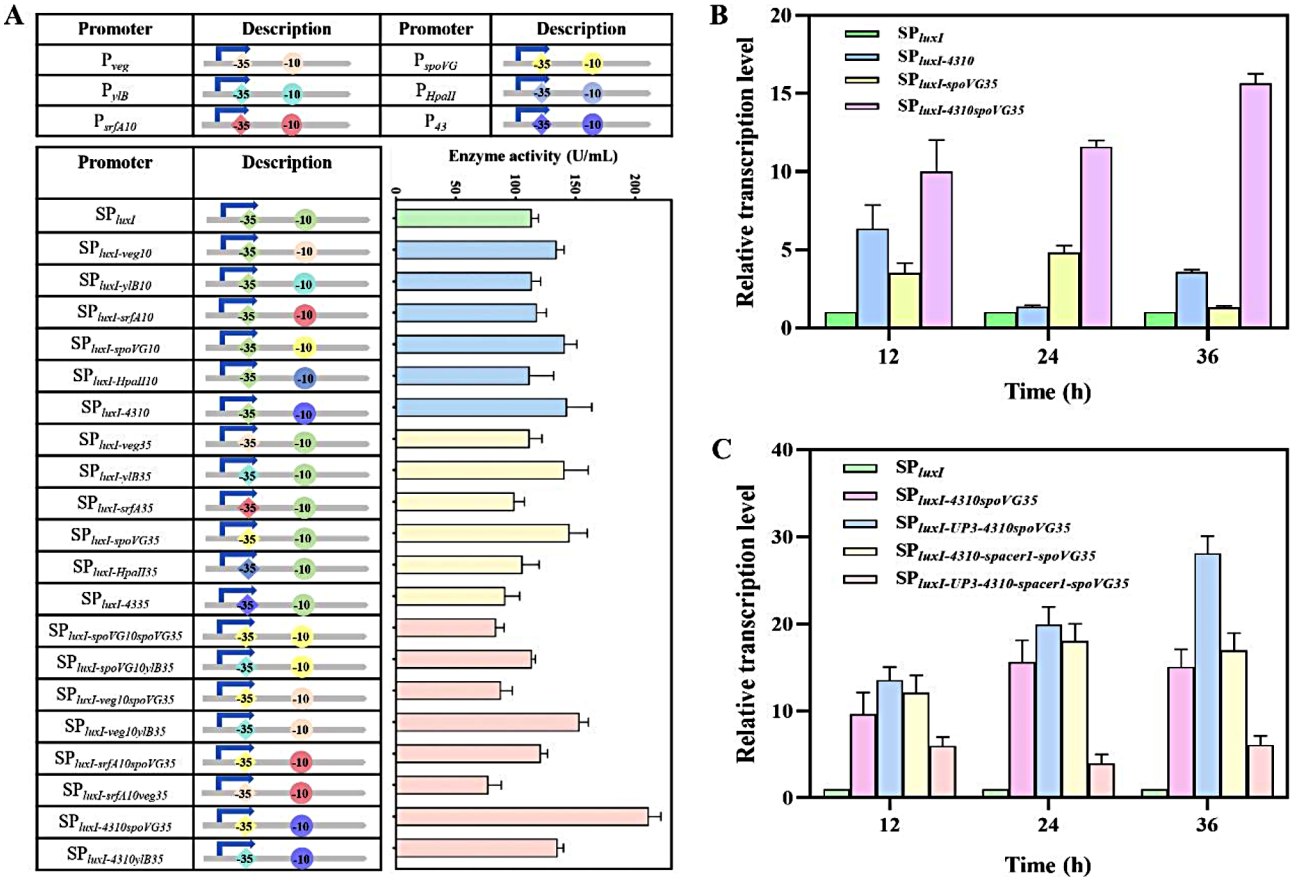

Fig. 3 Extracellular amylase activities and transcript levels produced by engineering the core region (−10 and −35) of SP_{luxI}. (**A**) Extracellular amylase activities generated by engineering the core region (−10 and −35) of SP_{luxI}. Enzyme activities generated by the same type of expression strategy are represented by the same colour. Transcript levels of *amyZ1* (**B**) and *luxI* (**C**) mediated by LuxI/R devices containing various SP_{luxI} core region mutants. The error bars represent the standard deviation

greater than those of the control SP_{luxI}, respectively. The mutants $SP_{luxI-spoVG35}$ and $SP_{luxI-ylB35}$ were obtained by replacing the − 35 region of P_{spoVG} and P_{ylB}, respectively. These mutants exhibited extracellular amylase activities of 141 and 140 U/mL (Fig. 3A), which were 1.23- and 1.22-fold greater than those of SP_{luxI}.

To further enhance the autoinducible expression of the *lux* system in *B. subtilis*, we performed a combined substitution based on individual substitutions in the − 10 and − 35 regions (Fig. 3A). The mutant $SP_{luxI-4310spoVG35}$, obtained by combined substitution of the − 10 region of P_{43} and the − 35 region of P_{spoVG}, exhibited an extracellular amylase activity of 210 U/mL. This activity was 1.83-, 1.47-, and 1.49-fold greater than that of SP_{luxI}, $SP_{luxI-4310}$, and $SP_{luxI-spoVG35}$, respectively (Fig. 3A). In a previous study, Corrêa et al. used a consensus sequence of the *B. subtilis* σ^A factor to replace the − 10 region of P_{luxI} in the response module [17]. The resulting mutant, R6, presented an approximately 2.6-fold increase in transcriptional activity compared with that of the control R4 [17]. However, Corrêa et al. did not investigate the underlying reason for the effects of the engineered response module P_{luxI} on the autoinducible expression of the *lux* system [17].

To elucidate the effect of engineering the core region of SP_{luxI} to enhance the autoinducible expression of the *lux* system, we determined the transcript levels of *amyZ1* mediated by the LuxI/R device containing SP_{luxI}, $SP_{luxI-4310}$, $SP_{luxI-spoVG35}$, and $SP_{luxI-4310spoVG35}$. As depicted in Fig. 3B, the *amyZ1* transcript levels mediated by $SP_{luxI-4310}$, $SP_{luxI-spoVG35}$, and $SP_{luxI-4310spoVG35}$ increased to varying degrees in shake flask fermentation compared with that mediated by the control, SP_{luxI}. This finding was consistent with the observed extracellular amylase activity. Among these constructs, $SP_{luxI-4310spoVG35}$ exhibited the highest transcriptional activity, which was 10–16 times greater than that of SP_{luxI}. Moreover, the level of *luxI* transcription mediated by $SP_{luxI-4310spoVG35}$ was greater than that mediated by SP_{luxI} throughout the culture period (Fig. 3C). Given these results, it was reasonable to speculate that the enhanced extracellular amylase activity observed after engineering the core region of SP_{luxI} may have been due to the heightened expression of *luxI* in the sensing module. This increase in expression led to a higher concentration of the signalling molecule AHL in the culture system. This further increased the content of the LuxR–AHL complex and the transcriptional activity of RP_{luxIR6}.

Engineering the UP region of $SP_{luxI-4310spoVG35}$

Structurally, some bacterial promoters contain two types of regions involved in RNAP recognition and binding: the classic core regions (− 10 and − 35) and the UP region [37]. The UP region is an AT-rich region located upstream of the promoter − 35 region with the sequence AAAWWTWTTTTNNNAAAN [38]. The UP region promotes the formation of the transcription initiation complex by binding to the α-subunit C-terminal structural domain (α-CTD) of RNAP, thereby increasing the transcriptional activity of the promoter [39]. Previously, by optimizing the UP region of P_{trxA}, Li et al. obtained the mutant P_{trxA}-UP5, which exhibited a 5.6-fold increase in transcriptional activity [39]. Phan et al. reported that, compared with the wild-type promoter P01 with a UP region, the promoter P70 lacking the UP region produced a 10-fold decrease in β-galactosidase activity, whereas the promoter P64 with a mutated UP sequence increased β-galactosidase activity by more than 2-fold [40]. In addition, Zhang et al. engineered the UP region sequence of P_{spovG} and demonstrated that three bases, AGC, upstream of the − 35 region, were the key bases influencing promoter transcriptional activity [41]. Removing these bases produced a 4.5-fold decrease in the GFP fluorescence intensity [41]. Overall, it can be inferred that manipulating the UP region is an effective engineering strategy for increasing the transcriptional activity of promoters.

Notably, there were no AT-rich UP regions present upstream of the − 35 region of $SP_{luxI-4310spoVG35}$ (Fig. 4A). To investigate the effect of the UP region on $SP_{luxI-4310spoVG35}$, we obtained three UP region sequences on the basis of previous reports and through rational design (Table 1). These sequences were then inserted upstream of the − 35 region of $SP_{luxI-4310spoVG35}$ to yield the mutants $SP_{luxI-UP1-4310spoVG35}$, $SP_{luxI-UP2-4310spoVG35}$, and $SP_{luxI-UP3-4310spoVG35}$. As shown in Fig. 4B, the extracellular amylase activities mediated by $SP_{luxI-UP1-4310spoVG35}$ and $SP_{luxI-UP2-4310spoVG35}$ were 142 and 144 U/mL, respectively, which were 68% and 69% that of $SP_{luxI-4310spoVG35}$. This inconsistency with the findings of Phan et al. may be due to differences in the sequences of the promoter core regions (− 10 and − 35) between the two studies [40].

The UP3 sequence with AGC inserted exhibited extracellular amylase activity mediated by $SP_{luxI-UP3-4310spoVG35}$ reaching 295 U/mL (Fig. 4B). This level was 1.4- and 2.6-fold greater than that of the control $SP_{luxI-4310spoVG35}$ and the original SP_{luxI}, respectively. This finding was consistent with the study by Zhang et al. and further demonstrated that the UP region crucially influences promoter transcriptional activity, particularly the AGC sequence located upstream of the − 35 region [41]. In addition, Li et al. noted that the UP region of the promoter could function independently of its core region [39]. They enhanced the transcriptional activity of P_{acpp} (which did not contain a UP region) 7.4-fold by inserting a UP region, generating UP5-2P [39].

To further investigate the cause of the increase in extracellular amylase activity mediated by the LuxI/R device

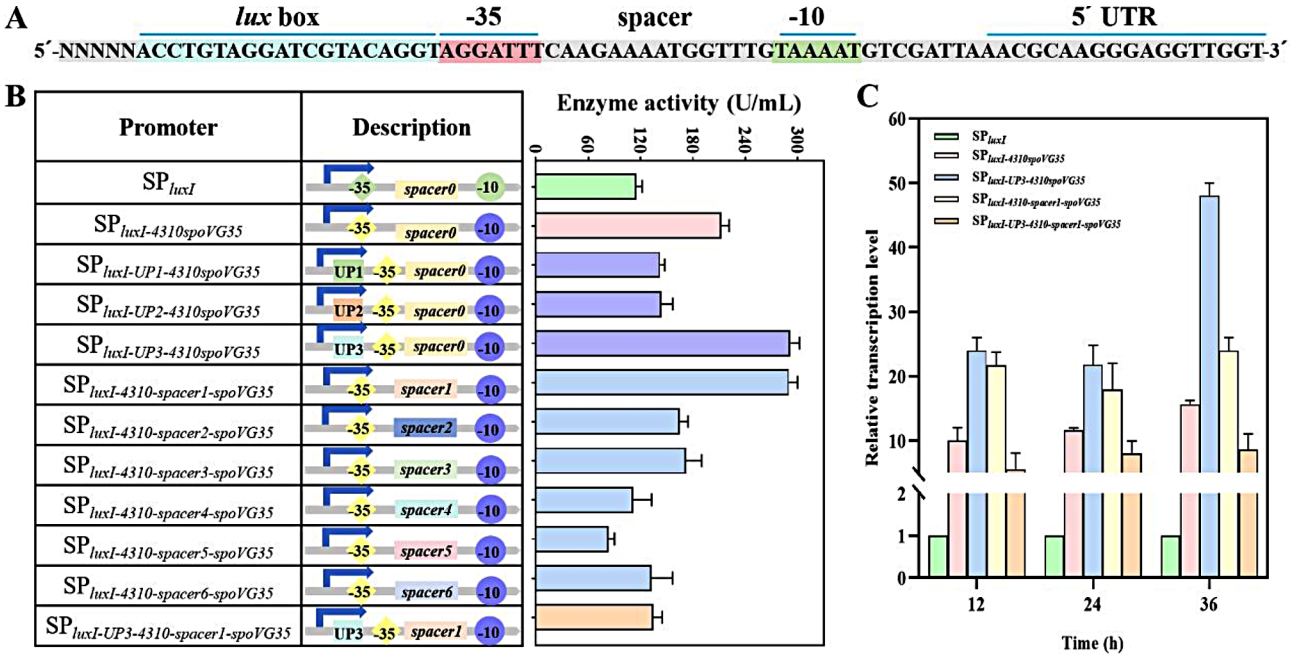

Fig. 4 Extracellular amylase activities and transcript levels produced by engineering the critical region (UP and spacer) of $SP_{luxI-4310spoVG35}$. (**A**) Sequence information for $SP_{luxI-4310spoVG35}$. (**B**) Engineering the UP and spacer regions of $SP_{luxI-4310spoVG35}$. (**C**) Transcriptional levels of *amyZ1* mediated by LuxI/R devices containing various $SP_{luxI-4310spoVG35}$ critical region mutants. The activities of enzymes generated by the same type of expression strategy are represented by the same colour. The error bars represent the standard deviation

Table 1 Sequence information for UP and spacer

Region	Sequence (5′-3′)	Source*
UP1	GGATCACTAGAAAATTTTTTAAAAAATCTC	[40]
UP2	GAGATTTTTTAAAAAATTTTCTAGTGATCC	[40]
UP3	AAAAATTTTTTAGCAAAGC	[38]
Spacer1	aaaagcgcgcgattatg	P_{43}
Spacer2	CAGAAAAAATCGTG	P_{spoVG}
Spacer3	caagaaaatgTATGT	AD
Spacer4	AAAACATTTTTTTCATT	P_{10}
Spacer5	aaagaaaatttttttg	AD
Spacer6	caaTaaaatTTtttg	AD

*AD indicates that the corresponding sequence was artificially designed in this study

containing $SP_{luxI-UP3-4310spoVG35}$, the transcript levels of *amyZ1* were measured. As shown in Fig. 4C, the transcriptional activity of $SP_{luxI-UP3-4310spoVG35}$ was 1.9–3.1 times greater than that of the control, $SP_{luxI-4310spoVG35}$. Moreover, the transcript level of *luxI* mediated by $SP_{luxI-UP3-4310spoVG35}$ was greater than that mediated by $SP_{luxI-4310spoVG35}$ (Fig. 4C). Thus, the increased extracellular amylase activity mediated by $SP_{luxI-UP3-4310spoVG35}$ may be attributed to the UP3 region, which promotes RNAP recruitment, leading to increased expression of *luxI* in the sensing module. Consequently, there was a further increase in the level of the LuxR–AHL complex and an increase in the transcriptional activity of RP_{luxIR6}.

Engineering the spacer region of $SP_{luxI-4310spoVG35}$

The spacer region located between the −10 and −35 regions of the promoter modulates the efficiency of σ factor recognition and binding by changing the conformation or curvature of the promoter [30]. The spacer regions are also critical in the subsequent structural regulation of the RNAP–DNA complex and in promoting open complex formation [7, 42]. Recent studies have indicated that the spacer region also interacts with the β-strand, an evolutionarily conserved loop of the RNAP subunit [43]. There have been numerous reports in which the spacer region was engineered to regulate promoter activity and the expression of target genes [44]. For example, Hwang et al. achieved a greater than 40-fold change in the fluorescence intensity of GFP in *Escherichia coli* by randomly mutating the spacer region of P_{nar} [45]. Similarly, Xu et al. achieved a 3.99-fold increase in the relative fluorescence intensity of sfGFP in *B. subtilis* by modifying the spacer region of P_{srfA} [13].

To investigate the impact of modifying the spacer region in $SP_{luxI-4310spoVG35}$, we semirationally replaced the original spacer region of $SP_{luxI-4310spoVG35}$ with those of P_{43} [33], P_{spoVG} [34], and P_{10} [46], which are strong promoters in the *B. subtilis* expression system. In addition, on the basis of the observation that a higher AT base content in the spacer region increased promoter activity [47], the spacer region of $SP_{luxI-4310spoVG35}$ was directionally mutated to increase its AT base content from 67 to

87%. A series of promoter mutants were ultimately constructed, as depicted in Table 1.

As shown in Fig. 4B, the extracellular amylase activity mediated by the LuxI/R device was reduced to varying degrees when spacers 2–6, but not spacer 1, were replaced. The extracellular amylase activity mediated by $SP_{luxI-4310-spacer5-spoVG35}$ was only 83 U/mL, which was 39.5% of that mediated by the control, $SP_{luxI-4310spoVG35}$ (Fig. 4B). In contrast, the extracellular amylase activity mediated by $SP_{luxI-4310-spacer1-spoVG35}$ after spacer 1 was replaced was 289 U/mL. This value was 1.38-fold greater than that for $SP_{luxI-4310spoVG35}$ and 2.51-fold greater than that for the original SP_{luxI}. This increase may be explained by spacer 1 being derived from P_{43}, with its number of bases (17 bp) being close to the theoretically optimal value (17–19 bp) [30]. This favoured RNAP binding to $SP_{luxI-4310spoVG35}$ to form a transcription initiation complex [42].

To investigate the effect of the combined UP and spacer region optimization on $SP_{luxI-4310spoVG35}$, the promoter mutant $SP_{luxI-UP3-4310-spacer1-spoVG35}$ was constructed using the optimal UP3 and spacer 1. Unexpectedly, $SP_{luxI-UP3-4310-spacer1-spoVG35}$ did not further increase extracellular amylase activity (Fig. 4B). Although the extracellular amylase activity mediated by $SP_{luxI-UP3-4310-spacer1-spoVG35}$ (135 U/mL) was 1.17-fold ($p < 0.05$) greater than that mediated by the original SP_{luxI}, the activity was 36%, 54%, and 53% lower than that mediated by $SP_{luxI-4310spoVG35}$, $SP_{luxI-UP3-4310spoVG35}$, and $SP_{luxI-4310-spacer1-spoVG35}$, respectively. As shown in Figs. 3C and 4C, the transcript levels of *amyZ1* and *luxI* mediated by $SP_{luxI-UP3-4310-spacer1-spoVG35}$ were lower than those mediated by $SP_{luxI-UP3-4310spoVG35}$, $SP_{luxI-4310-spacer1-spoVG35}$, and the control $SP_{luxI-4310spoVG35}$. These findings may be attributed to the spatial conformation of $SP_{luxI-UP3-4310-spacer1-spoVG35}$ containing UP3 exhibiting unfavourable binding to the α-CTD of RNAP after spacer 1 was replaced [39, 42]. This may have impeded the formation of the transcription initiation complex, ultimately reducing the concentration of the LuxR–AHL complex and the transcriptional activity of RP_{luxIR6}.

Engineering the core region of RP_{luxIR6}

Sequence optimization on the basis of the core and critical regions of SP_{luxI} (Figs. 3A and 4B) revealed that engineering the core region effectively enhanced the autoinducible expression of the *lux* system. To investigate the effect of the core region of the response module promoter RP_{luxIR6}, we first rationally modified the corresponding region of RP_{luxIR6} in the same manner in which the SP_{luxI} core region was modified, by individually replacing the corresponding regions of RP_{luxIR6} with the −10 and −35 regions of the promoters P_{ylB}, P_{HpaII}, P_{43}, P_{spoVG}, P_{veg}, and P_{srfA}. Unexpectedly, no positive results similar to those obtained with the SP modifications were obtained (data not shown).

In a previous study by Xu et al., the relative fluorescence intensity mediated by the mutant P1, obtained by random mutagenesis of the promoter P_{srfA}, was more than 1.87-fold greater than that mediated by the wild-type P_{srfA} [6]. Therefore, we modified the core region (−10 and −35) of RP_{luxIR6} using the concatenated primer NNNNNCAAGAAAATGGTTTGTTGNNNNNNN. High-throughput screening was then performed on the basis of the diameter of the transparent circles formed by the transformants on starch plates. Subsequently, rescreening was carried out via shake flask fermentation. After screening approximately 1600 transformants, a single transformant, WBLA1, with significantly higher extracellular amylase activity (216 U/mL, representing a 1.88-fold increase) than that of the control, WBLA, was identified. Further sequencing analysis revealed that the −35 region sequence of the WBLA1 response module promoter $RP_{luxIR6-GA}$ had mutated from the original TTTACG (in RP_{luxIR6}) to TTTACA.

In this study, RP_{luxIR6} originated from R6, previously reported by Corrêa et al. [17]. In their study, the −10 region sequence of R6, TATAGT, was replaced by the σ^A factor consensus sequence TATAAT. The −35 region sequence TTTACA of $RP_{luxIR6-GA}$ was more similar to the consensus sequence TTGACA of the *B. subtilis* σ^A factor than the TTTACG sequence of RP_{luxIR6}. Therefore, it was reasonable to attribute the higher extracellular amylase activity mediated by $RP_{luxIR6-GA}$ compared with RP_{luxIR6} to easier recognition and binding of $RP_{luxIR6-GA}$ to RNAP.

For convenience, in the subsequent experimental descriptions, the sensing modules containing SP_{luxI}, $SP_{luxI-UP3-4310spoVG35}$, $SP_{luxI-4310-spacer1-spoVG35}$, and $SP_{luxI-UP3-4310-spacer1-spoVG35}$ are referred to as S0, Sa, Sb, and Sc, respectively, and the response modules that contained RP_{luxIR6} and $RP_{luxIR6-GA}$ are referred to as R0 and R1, respectively. To investigate the effect of the combined sensing and response module optimization on the autoinducible expression of the *lux* system, the response module R1 was combined with the sensing modules Sa, Sb, and Sc to construct the LuxI/R devices Sa-R1 ($SP_{luxI-UP3-4310spoVG35}$-$RP_{luxIR6-GA}$), Sb-R1 ($SP_{luxI-4310-spacer1-spoVG35}$-$RP_{luxIR6-GA}$), and Sc-R1 ($SP_{luxI-UP3-4310-spacer1-spoVG35}$-$RP_{luxIR6-GA}$), respectively. The LuxI/R device based on SP_{luxI} and RP_{luxIR6} was named S0-R0 (SP_{luxI}-RP_{luxIR6}). After shake flask fermentation, the extracellular amylase activities mediated by Sa-R1, Sb-R1, and Sc-R1 were 182, 183, and 187 U/mL, respectively (Fig. 5A). The extracellular amylase activity mediated by Sc-R1 was 1.4-fold greater than that mediated by Sc-R0. However, the extracellular amylase

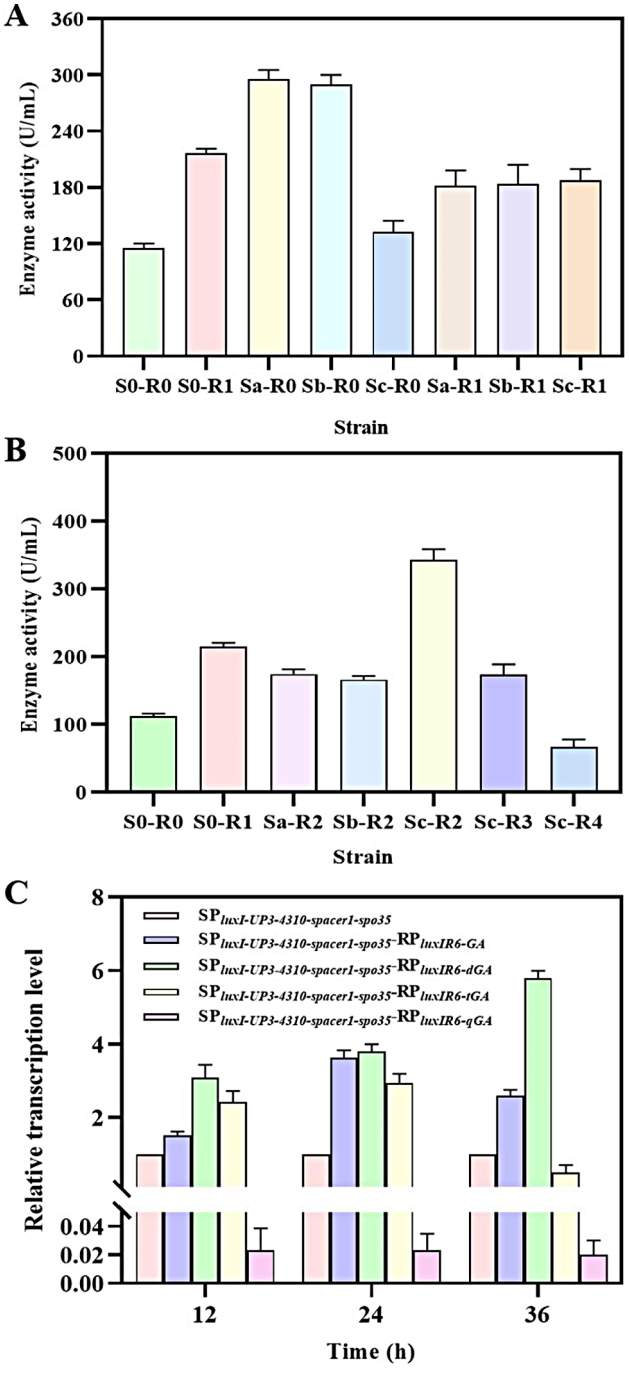

Fig. 5 Different LuxI/R devices mediate the extracellular expression of recombinant *amyZ1* in *B. subtilis*. (**A**) Recombinant extracellular amylase activity mediated by various LuxI/R devices containing R1. (**B**) Recombinant extracellular amylase activity mediated by LuxI/R devices with various *lux* box copy numbers. (**C**) Transcript levels of *amyZ1* mediated by LuxI/R devices with various *lux* box copy numbers. The different colours of the bars in the figure distinguish the different LuxI/R devices shown. The error bars represent the standard deviation

activities mediated by Sa-R1 and Sb-R1 were 61.7% and 63.3% those mediated by Sa-R0 and Sb-R0, respectively.

The autoinducible expression mechanism of the LuxI/R device was based on LuxR binding to AHL encoded by *luxI* to form the LuxR–AHL complex. This complex then bound to the *lux* boxes of SP_{luxI} and RP_{luxIR6}, thereby further enhancing the expression of *luxI* in the sensing module and *amyZ1* in the response module. When the transcriptional activity of both SP_{luxI} and RP_{luxIR6} was low, the autoinducible expression of the LuxI/R device increased as the transcriptional activity of SP_{luxI} and RP_{luxIR6} increased. This may explain why Sa-R0, Sb-R0, Sc-R0, and S0-R1 all presented higher extracellular amylase activities than did S0-R0. We inferred that due to the lower transcriptional activity of $SP_{luxI-UP3-4310-spacer1-spoVG35}$ than those of $SP_{luxI-UP3-4310spoVG35}$ and $SP_{luxI-4310-spacer1-spoVG35}$ (Fig. 3C), the intracellular concentration of the LuxR–AHL complex in Sc-R0 was low. Consequently, there was a reduction in AHL and AmyZ1 expression, leading to a decrease in extracellular amylase activity mediated by Sc-R0 compared with that mediated by Sa-R0 and Sb-R0.

In addition, owing to the greater transcriptional activity of R1 than of R0 (Fig. 5C), the *amyZ1* expression levels of Sa-R1 and Sb-R1 were greater than those of Sa-R0 and Sb-R0 when the cell concentration was relatively low. This led to an increased metabolic burden on cell growth, ultimately resulting in reduced AmyZ1 production. To investigate these hypotheses, we analysed the enzyme production profiles from shake flask fermentation of the recombinant strains using different LuxI/R devices. As shown in Additional file 1: Fig. S1 and 5 A, the OD_{600} and extracellular amylase activities of Sa-R1 and Sb-R1 were lower than those of Sa-R0 and Sb-R0, respectively, which aligned with our initial prediction.

However, independent of the LuxI/R devices based on the sensing modules for Sa and Sb, the extracellular amylase activity of Sc-R1 was greater than that of Sc-R0. This may have been due to the lower induction level of Sc than of Sa and Sb (Fig. 3C). Therefore, in contrast to Sa and Sb, the LuxI/R device containing Sc required a relatively high cell concentration to initiate *amyZ1* expression. This somewhat alleviated the inverse relationship between cell growth and product synthesis mediated by Sc-R1. In addition, the transcriptional activity of R1 was greater than that of R0 (Fig. 5C). Therefore, the extracellular amylase activity of Sc-R1 was greater than that of Sc-R0. This finding was consistent with the results shown in Additional file 1: Fig. S1, in which the OD_{600} of Sc-R1 did not change significantly compared with that of Sc-R0. Taken together, these results indicate that the extracellular amylase activity obtained from different LuxI/R devices is correlated with their ability to mitigate the trade-off between cell growth and protein synthesis.

Moreover, on the basis of this analysis, it was speculated that further increasing the response module activity of Sa-R1, Sb-R1, and Sc-R1 may result in increased extracellular amylase activity only for Sc-R1.

Engineering the *lux* box of $RP_{LuxIR6-GA}$

The LuxR–AHL complex binds to the *lux* box of P_{luxI}, promoting RNAP recruitment and thereby enhancing the expression of the *lux* system [18]. Ge et al. achieved a 2-fold change in the autoinducible expression of the *lux* system by designing a sequence spanning from the *lux* box to the −10 region of P_{luxI} [15]. Here, we investigated the effect of the *lux* box copy number of $RP_{luxIR6-GA}$ on the autoinducible expression of the *lux* system. $RP_{luxIR6-dGA}$ was obtained by adding a copy of the *lux* box to $RP_{luxIR6-GA}$, and its response module was designated R2. The LuxI/R devices constructed by combining R2 with the sensing modules Sa, Sb, and Sc were denoted Sa-R2, Sb-R2, and Sc-R2, respectively.

As shown in Fig. 5B, the extracellular amylase activities of Sa-R2, Sb-R2, and Sc-R2 were 174, 166, and 346 U/mL, respectively. Compared with Sc-R1, Sc-R2 exhibited 1.85-fold greater extracellular amylase activity. However, there was no significant difference ($p \geq 0.05$) in the extracellular amylase activity between Sa-R2 and Sa-R1 or between Sb-R2 and Sb-R1. This finding was consistent with the previous prediction that only the extracellular amylase activity of Sc-R1 would be further enhanced by an increase in the response activity of Sa-R1, Sb-R1, and Sc-R1. This may be attributed to the following reasons. First, R2 presented higher *amyZ1* expression than R1 did (Fig. 5C) because of an increase in the *lux* box copy number. Second, the LuxI/R device containing Sc exhibited a delay in the autoinducible expression of *amyZ1* compared with the devices containing Sa and Sb, which could mitigate the trade-off between cell growth and protein synthesis. To our knowledge, this is the first report in which the autoinducible expression of the *lux* system increased with increasing *lux* box copy number in the response module promoter.

Then, we constructed $RP_{luxIR6-tGA}$ and $RP_{luxIR6-qGA}$ by adding one and two copies of the *lux* box, respectively, to $RP_{luxIR6-dGA}$, and these were designated R3 and R4. After shake flask fermentation, the extracellular amylase activities of Sc-R3 and Sc-R4 were 173 and 67 U/mL (Fig. 5B), which were 50% and 19% that of Sc-R2, respectively. In addition, R3 and R4 presented lower *amyZ1* expression than R2 did ($p < 0.05$, Fig. 5C). This may have occurred because at high copy numbers, *lux* tended to bind the LuxR–AHL complexes, creating a barrier that hindered RNAP recognition and binding to the promoter, ultimately reducing AmyZ1 expression.

In a previous study of the endogenous Phr-Rap-type QS system in *B. subtilis*, Xu et al. reported that the transcriptional activity of the mutant $P_{spoiia\ (cs-3)}$, obtained by mutating the SpoOA binding site OA box in the promoter P_{spoIIA}, was 8-fold greater than that of wild-type P_{spoIIA} [48]. In addition, in a study by Ge et al., a mutant 43-QS system was obtained by replacing the sequence between the *lux* box and the −10 site in P_{luxI} of the *Vibrio* ES114 *lux* system with the corresponding sequence from the *Vibrio* MJ1 *lux* system. This modified system resulted in a fluorescence intensity in *B. subtilis* that was approximately 1.7-fold greater than that obtained with the original *Vibrio* ES114 *lux* system [15]. On the basis of these reports, engineering the *lux* box sequence of Sc-R2 is likely to be an effective strategy for further increasing the autoinducible expression of the *lux* system proposed in this study in *B. subtilis*, which warrants further research.

Generalizability and scale-up fermentation-based validation of the *B. subtilis* autoinducible extracellular expression system

Here, we aimed to assess the industrial application potential of the *B. subtilis* autoinducible expression system developed in this study by examining its generalizability and scale-up performance. First, the levansucrase BhLS 39 [49] and the invertase InvDz13 [26], which are known for their importance in soybean oligosaccharide and raffinose conversion, respectively, in industrial settings were used as novel reporter proteins for shake-flask fermentation using the same medium and culture conditions as those used for AmyZ1 to validate the generalizability of the expression system. Second, a 3-L fermenter was used to culture the recombinant strain regulated by P_{veg} and Sc-R2 to validate the scale-up feasibility of the expression system.

As shown in Fig. 6A, the extracellular enzyme activity mediated by Sc-R2 was 2.6-fold greater than that mediated by S0-R0 when either BhLS 39 or InvDz13 was used as a novel reporter protein. As shown in Fig. 6B, the maximum extracellular amylase activity and OD_{600} achieved with Sc-R2 were 5814.67 U/mL and 226.5, respectively, at 44 and 56 h during fermentation in the 3-L fermenter, while those for P_{veg} were 1892 U/mL and 197 at 32 and 60 h, respectively (Fig. 6B). The extracellular amylase activity, productivity, and OD_{600} mediated by Sc-R2 were 3.07-, 2.24-, and 1.15-fold greater, respectively, than those for P_{veg}. These results indicate that the *B. subtilis* autoinducible extracellular expression system regulated by Sc-R2 has good generalizability and scale-up fermentation potential. Similarly, in a study by Corrêa et al., the yield of vitamin B2 obtained with an optimized LuxI/R device, S1-R6, was approximately 1.9-fold greater than that for P_{veg} [15].

In conclusion, in addition to the LuxI/R device in *B. subtilis* mediating the production of high-value-added fine chemicals, it also facilitated extracellular protein

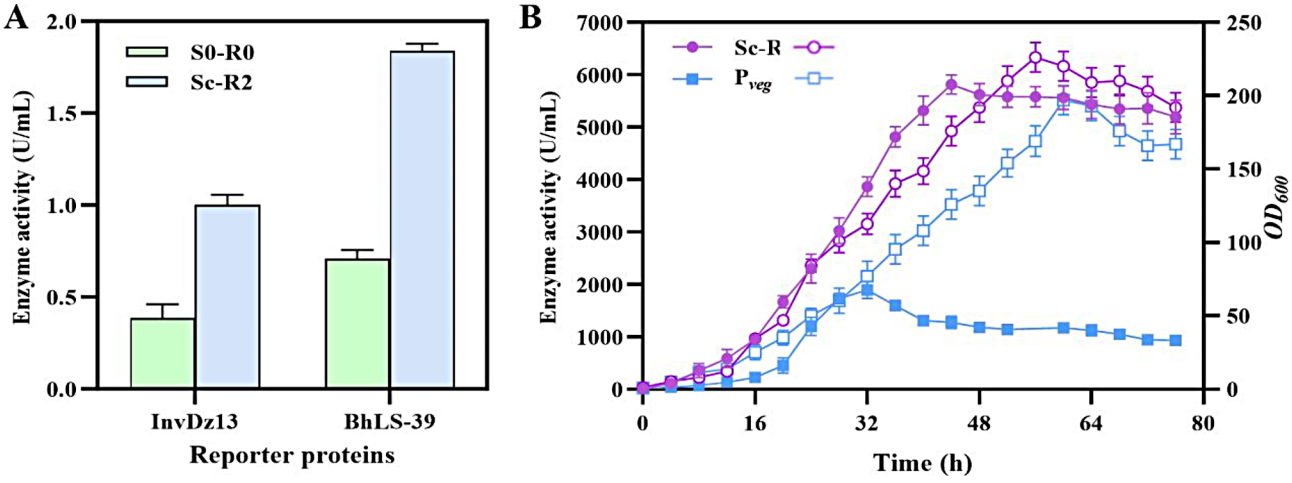

Fig. 6 Generalizability (**A**) and scale-up fermentation (**B**) validation of the *B. subtilis* autoinducible expression system. The solid line represents the enzyme activity, and the blank represents the OD_{600}. The error bars represent the standard deviation

expression. Previous studies have indicated that increasing LuxR expression in the sensing module and its binding affinity for AHL and the *lux* box effectively increased the autoinducible expression of the *lux* system in *E. coli* [19, 50]. However, there are no relevant reports on *B. subtilis*. Therefore, future studies can build upon LuxR to further increase the autoinducible expression of the *lux* system in *B. subtilis*, thereby improving the application value of the *B. subtilis* autoinducible expression system developed in this study. This study provides an effective microbial platform for protein expression and expands the application potential of QS-based autoinduction systems in *B. subtilis*.

Conclusion

A novel *B. subtilis* autoinducible extracellular expression system based on the LuxI/R device of *V. fischeri* was developed in this study. By engineering the sensing module and response module promoters of the LuxI/R device, the extracellular amylase activity mediated by the Sc-R2 system was 3.0-fold greater than that of the original S0-R0. To our knowledge, this study is the first to report the use of the LuxI/R device to mediate the recombinant extracellular expression of target proteins in *B. subtilis* and to increase the autoinducible expression of the *lux* system in *B. subtilis* by engineering its sensing module promoter and the *lux* box copy number of the response module promoter. Furthermore, the *B. subtilis* autoinducible extracellular expression system developed here exhibited good generalizability and application potential for industrial-scale fermentation. This study provides an effective microbial platform for protein expression and expands the application potential of QS-based autoinducible extracellular expression systems in *B. subtilis*.

Abbreviations

AHL	Acylhomoserine lactone
AIP	Autoinducible peptide
α-CTD	α-subunit C-terminal structural domain
DNS	3,5-dinitrosalicylic acid
GOI	Gene of interest
GRAS	Generally regarded as safe
lux system	LuxI/R-type system
POE-PCR	Prolonged overlap extension polymerase chain reaction
qRT–PCR	Quantitative real-time PCR
QS	Quorum sensing
RNAP	RNA polymerase
SDS–PAGE	Sodium dodecyl sulfate–polyacrylamide gel electrophoresis

Supplementary Information

The online version contains supplementary material available at https://doi.org/10.1186/s12934-025-02719-8.

Supplementary Material 1: **Additional file 1: Plasmid construction** Plasmid constructionPlasmid construction for the − 10 and − 35 region modifications in SP_{luxI}. Plasmid construction for the UP region modifications in SP_{luxI}. Plasmid construction for the spacer region modifications in SP_{luxI}. Plasmid construction for the core region modifications in RP_{luxIR6}. Plasmid construction for the ***lux*** box modifications in $RP_{luxIR6-GA}$. Plasmid construction for other reporter proteins. **Figure** Fig. S1 The cell density of recombinant strains mediated by various LuxI/R devices. **Tables** Table S1 Strains and plasmids used in this study. Table S2 Primers used in this study. Sequence information for the fragment $_{luxR}$-***luxR***-SP_{luxR}-SP_{luxI}-***luxI***-T_{ter}-RP_{luxIR6}. Sequence information for P_{veg}

Acknowledgements

Not applicable.

Author contributions

Bin Wang and Keyi Wang designed the project, carried out experiments, and drafted the manuscript. Xiuyue Zhao carried out experiments. Zemin Fang, Yanyan Zhao, and Yulu Fang revised the manuscript. Yazhong Xiao and Dongbang Yao supervised the project and revised the manuscript. All authors read and approved the final manuscript.

Funding

This work was supported by the National Natural Science Foundation of China (32302017), the National Key Research and Development Program of China (2022YFC2805102), the Anhui Provincial Association for Science and Technology Young Science and Technology Talent Support Programme Project (RCTJ202409), the Doctoral Research Start-up Funding of Anhui University (S020318003/006).

Data availability
No datasets were generated or analysed during the current study.

Declarations

Ethics approval and consent to participate
Not applicable.

Consent for publication
Not applicable.

Competing interests
The authors declare no competing interests.

Received: 21 October 2024 / Accepted: 11 April 2025
Published online: 19 April 2025

References

1. Wu Y, Li Y, Zhang Y, Liu Y, Li J, Du G, Lv X, Liu L. Efficient protein expression and biosynthetic gene cluster regulation in *Bacillus subtilis* driven by a T7-BOOST system. ACS Synth Biol. 2023;12:3328–39.
2. Zhang G, An Y, Zabed HM, Yun J, Parvez A, Zhao M, Zhang C, Ravikumar Y, Li J, Qi X. Rewiring *Bacillus subtilis* and bioprocess optimization for oxidoreductive reaction-mediated biosynthesis of D-tagatose. Bioresource Technol. 2023;389:129843.
3. Zhang W, Ren H, Chen J, Ni D, Xu W, Mu W. Enhancement of the D-allulose 3-epimerase expression in *Bacillus subtilis* through both transcriptional and translational regulations. J Agric Food Chem. 2024;72:8052–9.
4. Yuan P, Xu M, Mao C, Zheng H, Sun D. Dynamically regulating glucose uptake to reduce overflow metabolism with a quorum-sensing circuit for the efficient synthesis of d-pantothenic acid in *Bacillus subtilis*. ACS Synth Biol. 2023;12:2983–95.
5. Fu G, Yue J, Li D, Li Y, Lee SY, Zhang D. An operator-based expression toolkit for *Bacillus subtilis* enables fine-tuning of gene expression and biosynthetic pathway regulation. P Natl Acad Sci. 2022;119:e2119980119.
6. Xu K, Tong Y, Li Y, Tao J, Rao S, Li J, Zhou J, Liu S. Autoinduction expression modules for regulating gene expression in *Bacillus subtilis*. ACS Synth Biol. 2022;11:4220–5.
7. Put H, Gerstmans H, Capelle HV, Fauvart M, Michiels J, Masschelein J. *Bacillus subtilis* as a host for natural product discovery and engineering of biosynthetic gene clusters. Nat Prod Rep. 2024;41:1113–51.
8. Yao D, Han X, Gao H, Wang B, Fang Z, Li H, Fang W, Xiao Y. Enhanced extracellular production of Raw starch-degrading a-amylase in *Bacillus subtilis* through expression regulatory element modification and fermentation optimization. Microb Cell Fact. 2023;22:118.
9. Zhu X, Zhang K, Luo H, Wu J. Overexpression of the class a penicillin-binding protein PonA in *Bacillus* improves Recombinant protein production. Bioresource Technol. 2023;383:129219.
10. Abisado RG, Benomar S, Klaus JR, Dandekar AA, Chandler JR. Bacterial quorum sensing and microbial community interactions. mBio. 2018;9:10–1128.
11. Silva BF, Correa GG, Zocca VFB, Picheli FP, Lins MRCR, Pedrolli DB. Expanding the functionality of an autoinduction device for repression of gene expression in *Bacillus subtilis*. Int J Mol Sci. 2023;24:84.
12. Hu L-x, Zhao M, Hu W-s, Zhou M-j, Huang J-b, Huang X-l, Gao X-l, Luo Y-n, Li C, Liu K, et al. Poly-γ-glutamic acid production by engineering a DegU quorum-sensing circuit in *Bacillus subtilis*. ACS Synth Biol. 2022;11:4156–70.
13. Xu K, Tong Y, Li Y, Tao J, Rao S, Li J, Zhou J, Liu S. Efficient, flexible autoinduction expression systems with broad initiation in *Bacillus subtilis*. ACS Synth Biol. 2021;10:3084–93.
14. Mukherjee S, Bossier BL. Bacterial quorum sensing in complex and dynamically changing environments. Nat Rev Microbiol. 2019;17:371–82.
15. Ge C, Yu Z, Sheng H, Shen X, Sun X, Zhang Y, Yan Y, Wang J, Yuan Q. Redesigning regulatory components of quorum-sensing system for diverse metabolic control. Nat Commun. 2022;13:2182.
16. Liu H, Wang X, Yang S, Wang R, Wang T. Saturation mutagenesis and self-inducible expression of Trehalose synthase in *Bacillus subtilis*. Biotechnol Progr. 2019;35:e2826.
17. Correa GG, da Costa Ribeiro Lins MR, Silva BF, de Paiva GB, Bertolazzi Zocca VF, Ribeiro NV, Picheli FP, Mack M, Pedrolli DB. A modular autoinduction device for control of gene expression in *Bacillus subtilis*. Metab Eng. 2020;61:326–34.
18. Waters CM, Bassler BL. Quorum sensing: Cell-to-cell communication in bacteria. Annu Rev Cell Dev Biol. 2005;21:319–46.
19. Soma Y, Hanai T. Self-induced metabolic state switching by a tunable cell density sense for microbial isopropanol production. Metab Eng. 2015;30:7–15.
20. Kang X-M, Cai X, Huang Z-H, Liu Z-Q, Zheng Y-G. Construction of a highly active secretory expression system in *Bacillus subtilis* of a Recombinant amidase by promoter and signal peptide engineering. Int J Biol Macromol. 2020;143:833–41.
21. Zhou Z, Cui W, Hao W, Ye C, Han L, Liu Z, Zhou L, Guo J. An autoinduced gene expression system for *Bacillus subtilis* based on Lux population sensing elements. In *China Invention Patent*. China 2021.
22. Li H, Yao D, Ying J, Han X, Zhang X, Fang X, Fang Z, Xiao Y. Enhanced extracellular Raw starch-degrading α-amylase production in *Bacillus subtilis* through signal peptide and translation efficiency optimization. Biochem Eng J. 2022;189:108718.
23. Wu X-C, Lee W, Tran L, Wong S. Engineering a *Bacillus subtilis* expression-secretion system with a strain deficient in six extracellular proteases. J Bacteriol. 1991;173:4952–8.
24. Zhong C, You C, Wei P, Zhang Y-HP. Simple cloning by prolonged overlap extension-PCR with application to the Preparation of large-size random gene mutagenesis library in *Escherichia coli*. Synth DNA: Methods Protocols. 2017:49–61.
25. Li H, Yao D, Pan Y, Chen X, Fang Z, Xiao Y. Enhanced extracellular Raw starch-degrading α-amylase production in Bacillus subtilis by promoter engineering and translation initiation efficiency optimization. Microb Cell Fact. 2022;21:127.
26. Liu J, Cheng J, Huang M, Shen C, Xu K, Xiao Y, Pan W, Fang Z. Identification of an invertase with high specific activity for raffinose hydrolysis and its application in soymilk treatment. Front Microbiol. 2021;12:646801.
27. Livak KJ, Schmittgen TD. Analysis of relative gene expression data using real-time quantitative PCR and the $2^{-\Delta\Delta CT}$ method. Methods. 2001;25:402–8.
28. Gao G-R, Hou Z-J, Ding MZ, Bai S, Wei SY, Qiao B, Xu Q-M, Cheng J-S, Yuan Y-J. Improved production of Fengycin in *Bacillus subtilis* by integrated strain engineering strategy. ACS Synth Biol. 2022;11:4065–76.
29. Zhou C, Ye B, Cheng S, Zhao L, Liu Y, Jiang J, Yan X. Promoter engineering enables overproduction of foreign proteins from a single copy expression cassette in *Bacillus subtilis*. Microb Cell Fact. 2019;18:1–11.
30. Wang Y, Shi Y, Hu L, Du G, Chen J, Kang Z. Engineering strong and stress-responsive promoters in *Bacillus subtilis* by interlocking Sigma factor binding motifs. Syn Syst Biotechno. 2019;4:197–203.
31. Guan C, Cui W, Cheng J, Zhou L, Liu Z, Zhou Z. Development of an efficient autoinducible expression system by promoter engineering in *Bacillus subtilis*. Microb Cell Fact. 2016;15:1–12.
32. Yang H, Ma Y, Zhao Y, Shen W, Chen X. Systematic engineering of transport and transcription to boost alkaline α-amylase production in *Bacillus subtilis*. Appl Microbiol Biot. 2020;104:2973–85.
33. Niu J, Yan R, Shen J, Zhu X, Meng F, Lu Z, Lu F. Cis-element engineering promotes the expression of *Bacillus subtilis* type I L-asparaginase and its application in food. Int J Mol Sci. 2022;23:6588.
34. Gan T, Fang J, Wang Y, Liu K, Sang Y, Chen H, Lu Y, Zhu L, Chen X. Promoter engineering for efficient production of sucrose phosphorylase in *Bacillus subtilis* and its application in enzymatic synthesis of 2-O-a-D-glucopyranosyl-L-ascorbic acid. Enzyme Microb Tech. 2023;169:110267.
35. Castillo-Hair SM, Baerman EA, Fujita M, Igoshin OA, Tabor JJ. Optogenetic control of *Bacillus subtilis* gene expression. Nat Commun. 2019;10:3099.
36. Zhang W, Wei M, Sun X, Lu F, Guan L, Mao S, Qin H-M. Fine-tuning of carbon flux and artificial promoters in *Bacillus subtilis* enables high-level biosynthesis of D-allulose. J Agric Food Chem. 2022;70:13935–44.
37. Einav T, Phillips R. How the avidity of polymerase binding to the–35/–10 promoter sites affects gene expression. P Natl Acad Sci. 2019;116:13340–5.
38. Browning DF, Busby SJW. Local and global regulation of transcription initiation in bacteria. Nat Rev Microbiol. 2016;14:638–50.
39. Li Y, Ma X, Zhang L, Ding Z, Xu S, Gu Z, Shi G. Engineering of *Bacillus* promoters based on interacting motifs between UP elements and RNA polymerase (RNAP) α-subunit. Int J Mol Sci. 2022;23:13480.
40. Trang Thi Phuong P, Hoang Duc N, Schumann W. Development of a strong intracellular expression system for *Bacillus subtilis* by optimizing promoter elements. J Biotechnol. 2012;157:167–72.

41. Zhang L, Liu P, Wang Y, Du G, Kang Z. Engineering and characterization of *Bacillus subtilis* P_{spovG} promoter. J Food Sci Biotech. 2022;41:20–7.
42. Forquet R, Nasser W, Reverchon S, Meyer S. Quantitative contribution of the spacer length in the supercoiling-sensitivity of bacterial promoters. Nucleic Acids Res. 2022;50:7287–97.
43. Klein CA, Teufel M, Weile CJ, Sobetzko P. The bacterial promoter spacer modulates promoter strength and timing by length, TG-motifs and DNA supercoiling sensitivity. Sci Rep. 2021;11:24399.
44. Xu J, Liu X, Yu X, Chu X, Tian J, Wu N. Identification and characterization of sequence signatures in the *Bacillus subtilis* promoter P_{ylb} for tuning promoter strength. Biotechnol Lett. 2020;42:115–24.
45. Hwang HJ, Lee SY, Lee PC. Engineering and application of synthetic Nar promoter for fine-tuning the expression of metabolic pathway genes in *Escherichia coli*. Biotechnol Biofuels. 2018;11:1–13.
46. Cheng J, Guan C, Cui W, Zhou L, Liu Z, Li W, Zhou Z. Enhancement of a high efficient autoinducible expression system in *Bacillus subtilis* by promoter engineering. Protein Expres Purif. 2016;127:81–7.
47. Deng C, Li J, Shin H-d, Du G, Chen J, Liu L. Efficient expression of cyclodextrin glycosyltransferase from *Geobacillus stearothermophilus* in *Escherichia coli* by promoter engineering and downstream box evolution. J Biotechnol. 2018;266:77–83.
48. Cui S, Lv X, Wu Y, Li J, Du G, Ledesma-Amaro R, Liu L. Engineering a bifunctional Phr60-Rap60-Spo0A quorum-sensing molecular switch for dynamic fine-tuning of menaquinone-7 synthesis in *Bacillus subtilis*. ACS Synth Biol. 2019;8:1826–37.
49. Wang B, Ying J, Chen Y, Fang Z, Xiao Y, Fang W, Yao D. Mining, characterization, and expression of a Fructan sucrase for efficient conversion of soybean oligosaccharides. Chin J Biotechnol. 2024;In press:1–19.
50. He X, Chen Y, Liang Q, Qi Q. Autoinduced and gate controls metabolic pathway dynamically in response to microbial communities and cell physiological state. ACS Synth Biol. 2017;6:463–70.

Publisher's note